Simulating Reinforced Concrete Beam-Column Against Close-In Detonation using S-ALE Solver

Shih Kwang Tay, Roger Chan and Jiing Koon Poon

Ministry of Home Affairs, Singapore

1 Abstract

A 3-stage loading on a reinforced concrete beam-column involving pre-load, blast and post-blast compression to failure was analyzed with the S-ALE solver. This paper presents the findings from the simulation and the results were compared to full-scale blast trials of reinforced concrete beam-column test specimens.

2 Introduction

Given the highly non-uniform blast loading during close-in detonation, structural response calculations using analytical methodologies such as Single-Degree-Of-Freedom (SDOF) would be beyond its applicable limits. From a design point of view, codes such as ASCE Standard 59-11 generally allow advanced non-linear finite element analyses for predicting close-in scenarios that involved complex structural response, localized shearing and breaching.

Unlike SDOF methodology that has established response limits such as support rotation to determine the corresponding component damage, designing structural elements against close-in detonation to an acceptable level of protection using numerical simulation is not a straight-forward task. For close-in or contact detonation, there will be significant localized damage due to the cratering and spalling, as shown by the column in Figure 1, and it is difficult to tell if the component is still able to carry the service load. As such, a quantitative measurement, such as the residual post-blast axial capacity, is required to determine the post-blast component performance.

Fig.1: Severely damaged column due to contact charge

A blast trial was conducted to investigate the residual axial capacity of reinforced concrete column (RC) subjected to close-in detonation. LS-DYNA simulations were performed using a development version of LS-DYNA Euler solver (ls-dyna_mpp_d_Dev_110107_winx64) for both the blast wave (loading) and RC structure (response).

For such close-in blast cases where severe deformation of the target is expected, past attempts to use Lagrangian models showed that there would be severe hourglassing of the elements, resulting in unrealistic energy balances. In addition, there is a need to correct material leakages into the

Lagrangian elements so as to ensure proper Fluid-Structure Interaction (FSI) between the Lagrange structure and detonation products. Both issues render the credibility of the modeling results questionable. As such, a pure Eulerian model which incorporated the explosive, air and structure was chosen to avoid the above issues.

This paper presents the use of Eulerian solver to simulate a structural response under a close-in blast loading using concrete model *MAT_SOIL_AND_FOAM (*MAT_005), *MAT_ELASTIC_PLASTIC_HYDRO (*MAT_010) and *MAT_PSEUDO_TENSOR (*MAT_016) and the results are compared to the experiments. The behavior of these three concrete models against dynamic loading were also studied in a separate paper [1].

3 Test Setup Overview

The RC column was positioned horizontally on support structures at a scaled distance Z = 0.8 m/kg$^{1/3}$, within close-in design range (Z < 1.2 m/kg$^{1/3}$) as defined in Unified Facilities Criteria (UFC) 3-340-02 [2]. The main charge was a spherical TNT charge, with the centre of the sphere raised to a height of 450 mm from the ground. The test specimen was a 300 mm x 300 mm square RC column with a clear span of 3m fixed with 500 mm x 700 mm x 500 mm RC blocks at both ends, as shown in Figure 2.

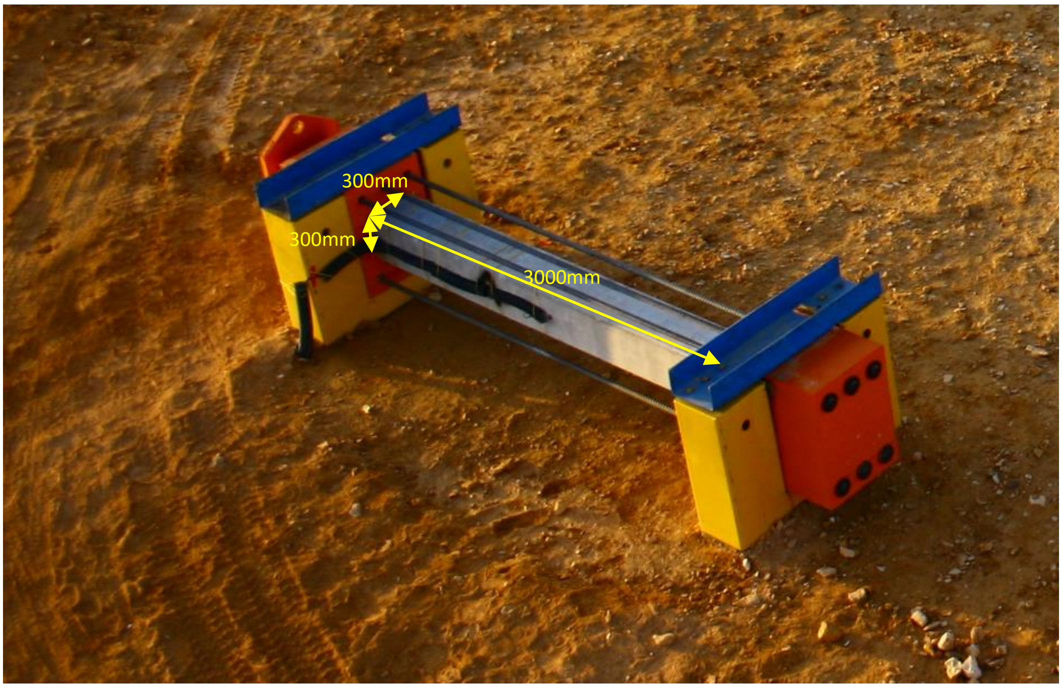

Fig.2: Test Column

The column was supported at the end blocks using a steel encased RC support structure. A 50-ton pre-load was applied and sustained to the column using a hydraulic jack. The residual axial capacity of the damaged column was measured in-situ using a compression rig after the blast.

4 Model Setup

The model was generated using *ALE_STRUCTURED_MESH and *INITIAL_VOLUME_FRACTION_GEOMETRY to invoke the Structured ALE (S-ALE) solver without the use of pre-processing software (See Appendix). *PARAMETER keyword also allowed the model to be quickly setup for parametric and mesh size study. Different views of the model consisting of air and the RC column are shown in Figures 3 to 5. The reinforcing bars and stirrups were modeled using one-dimensional beam elements and coupled to the concrete material using *ALE_COUPLING_NODAL_CONSTRAINT. Figure 6 shows the model of the rebars and stirrups.

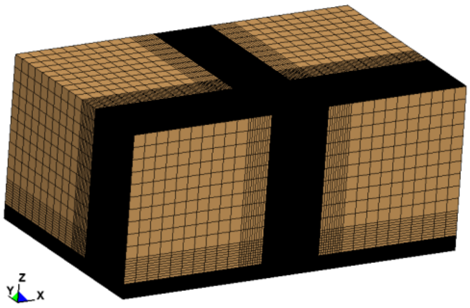

Fig.3: Mesh View

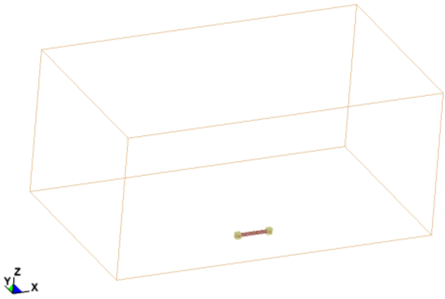

Fig.4: Wireframe View

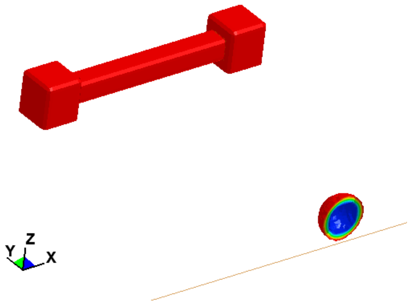

Fig.5: Volume Fraction with Iso-Surface

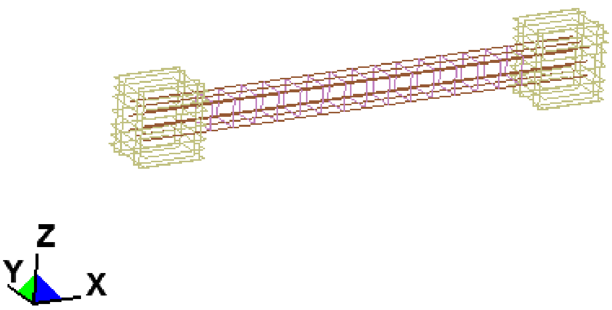

Fig.6: Model of the rebars and stirrups

Material

The material models selected for the runs were simple geomaterial models, *MAT_005, *MAT_010 and *MAT_016, calibrated to 32MPa unconfined compressive strength. The concrete material inputs can be found in the Appendix. Unlike other simple input concrete models such as *MAT_016, *MAT_072R3 and *MAT_159 which only requires minimal user input to invoke the auto generated parameters, *MAT_005 and *MAT_010 require the coefficients a_0, a_1 and a_2 to be calibrated to tri-axial compression data. The tri-axial test compression data were simulated with autogenerated *MAT_072R3. A trilinear equation-of-state *EOS_TABULATED_COMPACTION (*EOS_008) autogenerated with *MAT_072R3 was used with *MAT_010.

*MAT_016 Mode II concrete was used which included a damaged surface and damage scaling table based on parameters suggested in LS-DYNA User Manual [3] which are referenced to Dilger, Koch and Kowalczyk [1984] plain concrete.

$$a_{0f} = \frac{f_c^1}{10} \quad \text{and} \quad a_{1f} = 1.5$$

Card 4:	0.0	8.62E-06	2.15E-05	3.14E-05	3.95E-04
	5.17E-04	6.38E-04	7.98E-04		
Card 5:	9.67E-04	1.41E-03	1.97E-03	2.59E-03	3.27E-03
	4.00E-03	4.79E-03	0.909		
Card 6:	0.309	0.543	0.840	0.975	1.000
	0.790	0.630	0.469		
Card 7:	0.383	0.247	0.173	0.136	0.114
	0.086	0.056	0.0		

The reinforcement bars were defined using ELFORM=1 (Hughes-Liu) beam elements and *MAT_024 (Piecewise_Linear_Plasticity) was used as the constitutive model with *DEFINE_TABLE to specify the effective plastic strain values vs effective stress values at various strain rates.

Stages of Loading

The loadings were carried out in three stages. In the first stage, the column was axially compressed on one end and fixed on the other so as to achieve a pre-defined 50-ton pre-load. In the second stage, a spherical TNT resting on ground was detonated and the blast wave was allowed to propagate and impinge on the column. Post-blast compression to failure was conducted in the final stage to determine the residual capacity of the column.

Besides capturing the post-blast residual axial capacity, the original axial capacity of the reinforced concrete column model (not subjected to blast) was separately computed for the three material models by applying an axial compression load to failure. The results were compared to the actual control column compression result.

Boundary Conditions

The axial compression load was read using the nodal forces computed at the fixed end (Node Set 1001) of the concrete column. The keyword *DATABASE_NODAL_FORCE_GROUP allows the nodal forces to be aggregated easily to determine the total axial load applied to the concrete column.

The centre of charge was positioned on the –Y face of the generated structured mesh and raised 450 mm above ground (–Z face). Appropriate boundary conditions using *BOUNDARY_SPC were applied in the direction perpendicular to its face to represent the symmetry on the –Y face and reflecting ground on the –Z face as shown in the following keywords.

```
*SET_NODE_GENERAL
$      SID
      1001
$   OPTION        E1
       BOX         1
     DPART        23
*SET_NODE_GENERAL
$ Symmetry on -y face
$      SID
      1010
$   OPTION        E1        E2        E3        E4        E5        E6        E7
   SALEFAC         1                             1
*SET_NODE_GENERAL
$ Ground on -z face
$      SID
      1011
$   OPTION        E1        E2        E3        E4        E5        E6        E7
   SALEFAC         1                                                 1
*BOUNDARY_SPC_SET
$ NID/NSID       CID      DOFX      DOFY      DOFZ     DOFRX     DOFRY     DOFRZ
      1001         0         1         1         1         0         0         0
      1010         0         0         1         0         0         0         0
      1011         0         0         0         1         0         0         0
```

<u>Axial Compression</u>

Axial compression was applied by selecting a group of concrete only nodes within the end block and assigning *BOUNDARY_PRESCRIBED_MOTION at a constant velocity of 0.015 mm/ms towards the fixed end. The load was applied at a strain rate of 0.005 s^{-1} to simulate a quasi-static compressive load.

5 Results and Discussions

<u>Reference Column Comparison</u>

Compression test was performed on the model to obtain the axial capacity of the undamaged column. The results were compared with the actual control column which achieved an axial load capacity of 340 tons. Mesh sensitivity was investigated using three different mesh sizes (20mm, 30mm and 50mm). The results are shown in Figures 7, 8 and 9.

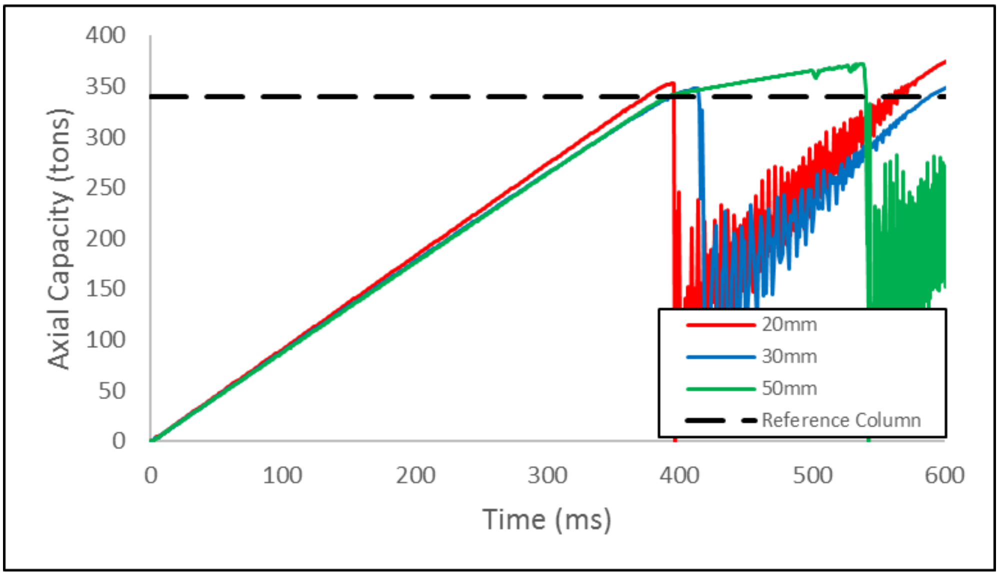

*Fig.7: Compression test result (*MAT_005)*

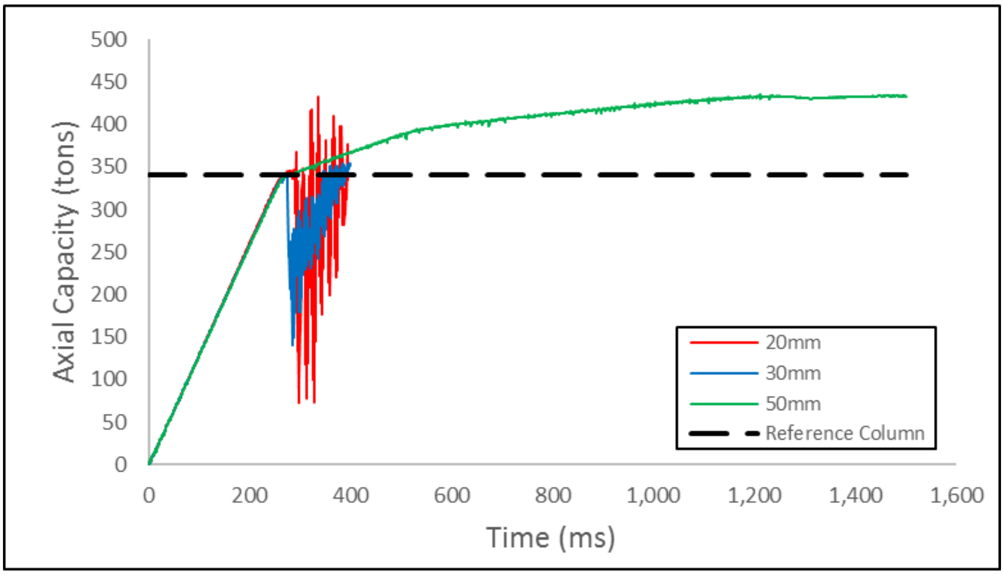

*Fig.8: Compression test result (*MAT_010)*

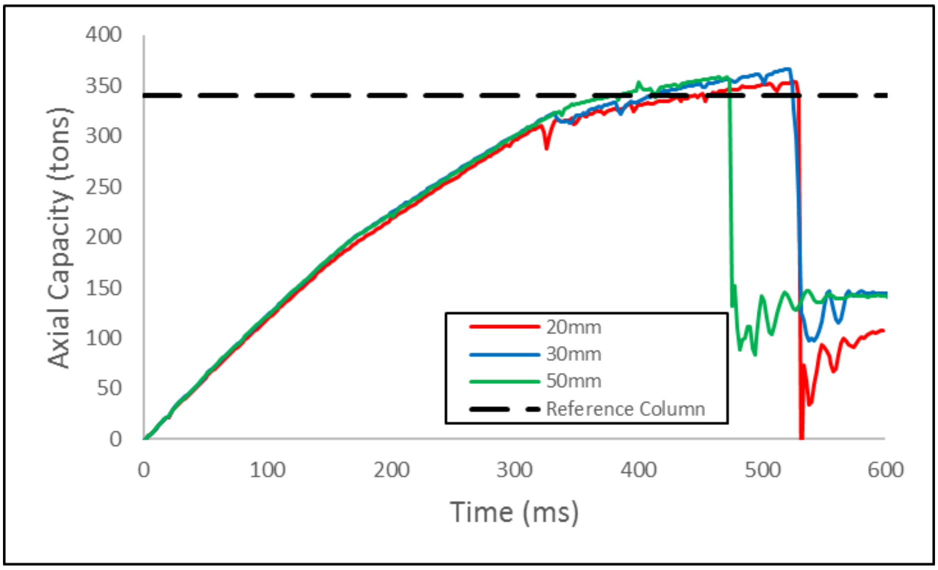

*Fig.9: Compression test result (*MAT_016)*

Material Model	Compressive Load (tons)			
	50mm	30mm	20mm	(Test data) Control Column
*MAT_005	371	346	352	340
*MAT_010	433	340	342	
*MAT_016	358	367	353	

Table 1: Summary of compressive load achieved by various models

It was demonstrated that the axial capacities of these Eulerian concrete models, when loaded in a quasi-static manner, were quite close to the actual experimental result. This lent confidence that the post blast axial compression will yield meaningful results. In addition, for all material models, the results were closer to that of the actual control column when the mesh was finer.

Comparison of Deflection

Although it was highlighted at the beginning of the paper, the support rotation for such close-in blast cases may not be a representative measurement of the component damage, it is nevertheless still useful as an additional parameter to assess the model's accuracy in predicting the experimental results.

In the experiment, the test column measured a permanent deflection of 94mm at midspan. A diagonal shear failure was also observed at one end of the column. In the numerical simulation, the horizontal deflections at midspan of the models were captured using *DATABASE_TRACER (TRACK=0) and compared against the test column as shown in Table 2.

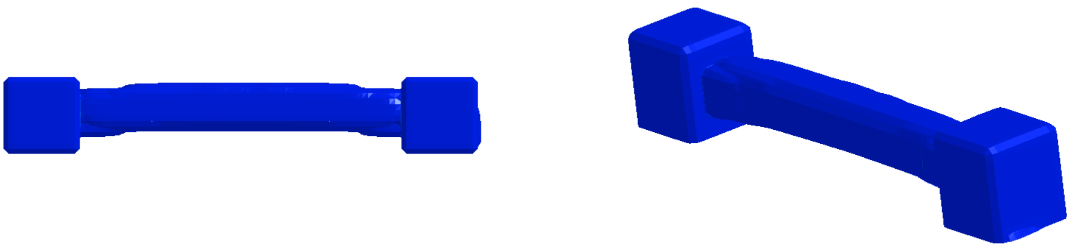

Fig.10: Blast loaded RC column (volume fraction with iso-surface)

Fig.11: Damaged Test Column

Material Model	Permanent Deflection (mm)		
	50mm	30mm	Test measurement
*MAT_005	70	63	94
*MAT_010	24	11	
*MAT_016	80	61	

Table 2: Summary of permanent deflection achieved by various models

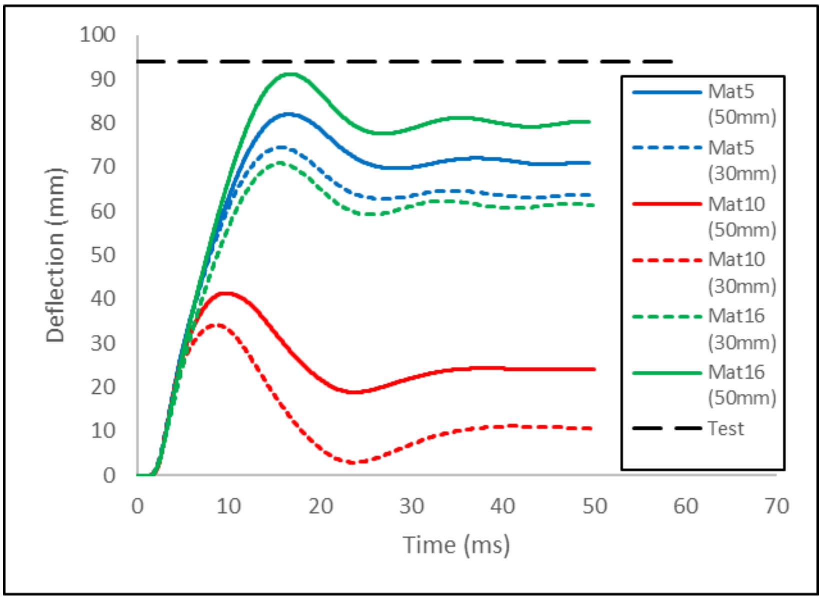

Fig.12: Midspan Deflection

It was observed that *MAT_005 and *MAT_016 were able to predict the flexural response of the actual column more closely as compared to *MAT_010. The 30mm mesh model using *MAT_010 only achieved approximately 10% of the actual midspan deflection.

<u>Residual Capacity</u>

The residual axial capacity of the test column was measured in-situ using a compression rig that was seated on the support structures. The test column measured a maximum load of only 12.5 ton due to the rebars buckling at the diagonal shear failure zone.

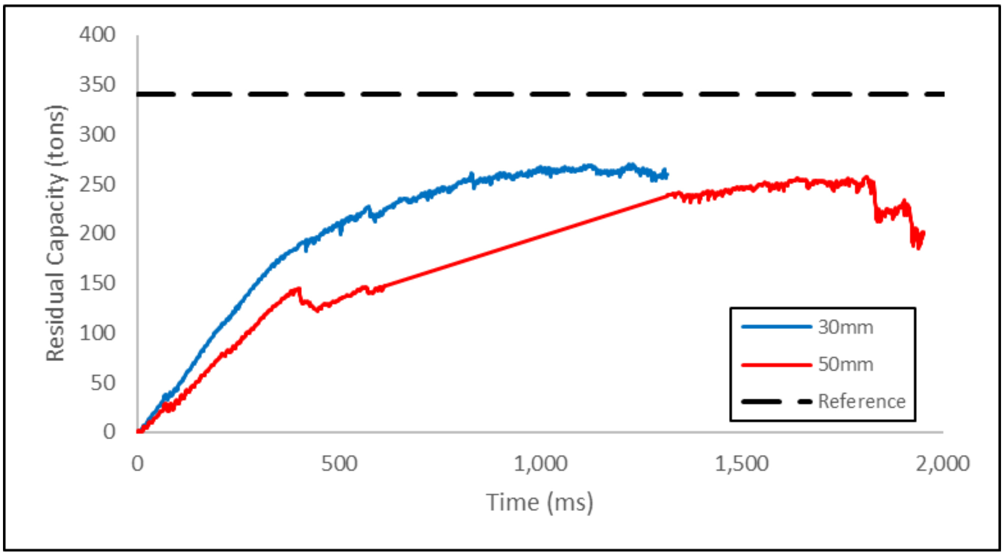

*Fig.13: Residual axial capacity (*MAT_005)*

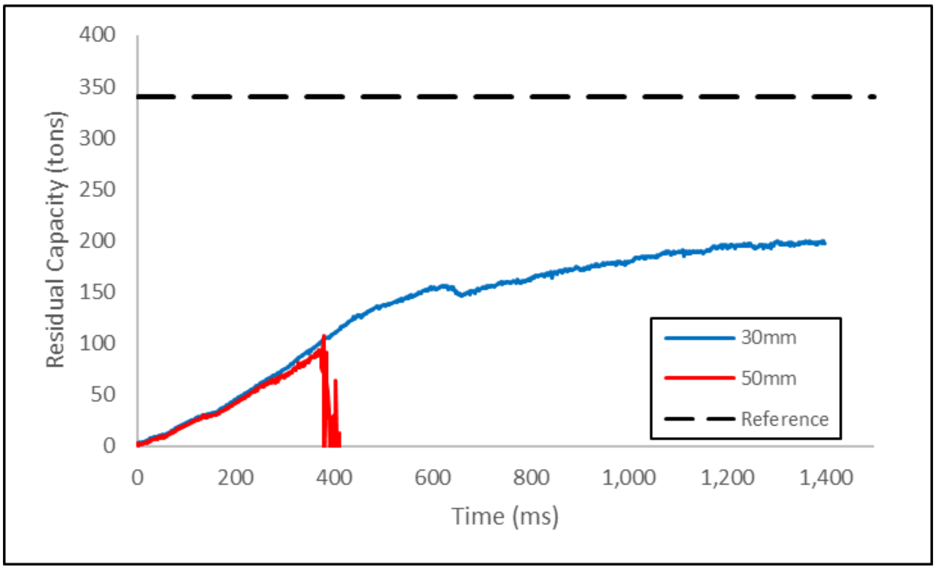

*Fig.14: Residual axial capacity (*MAT_010)*

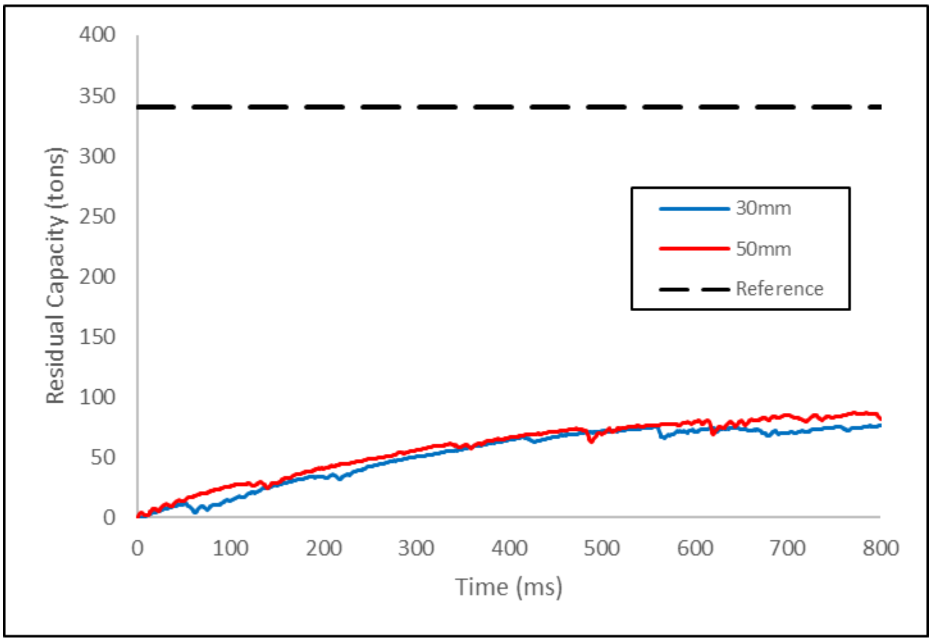

*Fig.15: Residual axial capacity (*MAT_016)*

Material Model	Residual Capacity (tons)		
	50mm	30mm	Test measurement
*MAT_005	252	265	12.5
*MAT_010	91	198	
*MAT_016	86	76	

Table 3: Summary of residual capacity achieved by various models

The 50 mm mesh model using *MAT_010 was observed to be unstable where the timestep drops rapidly at about 400ms and had to be terminated. Further mesh refinement at 30 mm mesh improved the stability and achieved maximum residual capacity of 198 tons.

The *MAT_005 and *MAT_010 models (30mm mesh) observed approximately 22-42% reduction in axial capacity although the test measured almost 96% reduction. *MAT_016 model on the other hand measured approximately 78% reduction of the axial capacity.

The close-in blast led to significant localized damage of the concrete and flexural response in the column. As expected from *MAT_005 and *MAT_010 where only the shear failure and pressure-volume surfaces are defined, the extent of damage to the concrete material will not be captured by these simple concrete models in a staged loading simulation. This was rightfully so as these constitutive models do not have any damage scaling and/or failure models incorporated in them. The blast loaded column will therefore still develop its strength based on the defined two-surface model (shear failure and pressure-volume surface) as though undamaged by the blast load during the post-blast compression. The reduced axial capacity observed for *MAT_005 and *MAT_010 models was likely due to buckling as a result of the flexural response in the column.

The *MAT_016 Mode II concrete on the other hand took into account the damage incurred during the blast loading and the subsequent post-blast compression more appropriately represented the reduced strength of the column through damage scaling. Having said that, the loss of concrete associated with localized cratering of concrete due to close-in air blast remains a concern and may not be possible to represent in these material models.

6 Conclusion

As mentioned in the introduction, the primary motivation for exploring the use of a full Eulerian model to simulate structural response in close-in detonation as an alternative to FSI using a Lagrangian model in Eulerian fluid space was to avoid issues associated with hourglassing and material “leakages”. This study has shown that the full Eulerian model exhibited reasonable results based on the selected material models.

The results presented in this paper also offers useful insights to the various concrete material models that support MM-ALE solid element formulation and the associated techniques to simulate such complex structural response against close-in scenario using a full Eulerian model. Based on the three material models investigated, although none of the models attained a post-blast axial capacity close to that obtained from the experiment, the result for *MAT_016 (Mode II) was the closest. This could be due to the material model having the capability to register damage due to the blast load, and this is important when performing a staged loading simulation.

7 References

[1] Jiing Koon Poon, Shih Kwang Tay, Roger Chan, Len Schwer. “Simulating Dynamic Loads on Concrete Components using the MM-ALE (Eulerian Solver)”, European LS-DYNA Conference, 2017.

[2] Structures to Resist the Effects of Accidental Explosions. Unified Facilities Criteria UFC 3-340-02, 2014.

[3] LS-DYNA R8.0 Keyword User’s Manual II, 2015.

Appendix

```
*ALE_STRUCTURED_MESH
$#   mshid       pid      nbid      ebid
         1      1001  50000001  50000001
$#   cpidx     cpidy     cpidz      nid0     lcsid
      2001      2002      2003
*ALE_STRUCTURED_MESH_CONTROL_POINTS
$ X-Dir
      2001
$#                x1                  x2
                   1            &xbound1
                  11            &xbound2
                  21                 &x1
             &xnode1                 &x2
             &xnode2            &xbound3
             &xnode3            &xbound4
*ALE_STRUCTURED_MESH_CONTROL_POINTS
$ Y-Dir
      2002
$#                x1                  x2
                   1                 &y1
             &ynode1                 &y2
             &ynode2            &ybound1
             &ynode3            &ybound2
*ALE_STRUCTURED_MESH_CONTROL_POINTS
$ Z-Dir
      2003
$#                x1                  x2
                   1                 &z1
             &znode1                 &z2
             &znode2            &zbound1
             &znode3            &zbound2
*INITIAL_VOLUME_FRACTION_GEOMETRY
$#   fmsid   fmidtyp     bammg    ntrace
      1001         1         2
$ Spherical Charge
$#  cnttyp   fillopt     fammg        vx        vy        vz
         6         0         1         0         0         0
$#      x0        y0        z0        r0
       &x0       &y0       &z0   &radius
$ Column
$# conttyp   fillopt     fammg        vx        xy        xz    radvel    unused
         5         0         3       0.0       0.0       0.0         0
$#    xmin      ymin      zmin      xmax      ymax      zmax    unused    unused
      &cx0      &cy0      &cz0      &cx1      &cy1      &cz1
$ End Block 1
$# conttyp   fillopt     fammg        vx        xy        xz    radvel    unused
         5         0         3       0.0       0.0       0.0         0
$#    xmin      ymin      zmin      xmax      ymax      zmax    unused    unused
    &eb1x0    &eb1y0    &eb1z0    &eb1x1    &eb1y1    &eb1z1
$ End Block 2
$# conttyp   fillopt     fammg        vx        xy        xz    radvel    unused
         5         0         3       0.0       0.0       0.0         0
$#    xmin      ymin      zmin      xmax      ymax      zmax    unused    unused
    &eb2x0    &eb2y0    &eb2z0    &eb2x1    &eb2y1    &eb2z1
*ALE_COUPLING_NODAL_CONSTRAINT_ID
$#  coupid
         1
$#   slave    master     stype     mtype     ctype     mcoup
        12      1001         0         1         2         0
$#   start       end                                  frcmin
     0.0001.0000E+10         0         0         0  0.500000
*SET_PART_LIST_TITLE
Rebars
$#     sid       da1       da2       da3       da4    solver
        12       0.0       0.0       0.0       0.0MECH
$#    pid1      pid2      pid3      pid4      pid5      pid6      pid7      pid8
        21        22        23         0         0         0         0         0
```

*MAT_005

```
*MAT_SOIL_AND_FOAM
$#     mid        ro         g      bulk        a0        a1        a2        pc
         3 2.1200E-3 11157.167 74381.227 26.268059 16.816317  1.189408 -1.010000
$#     vcr       ref      lcid
     0.000     0.000         0
$#    eps1      eps2      eps3      eps4      eps5      eps6      eps7      eps8
     0.000 5.7300E-2 9.4800E-2  0.111600  0.128700  0.145500  0.162600  0.177600
$#    eps9     eps10
  0.189000  0.211800
$#      p1        p2        p3        p4        p5        p6        p7        p8
     0.000 250.00000 500.00000 1000.0000 1500.0000 2000.0000 2500.0000 3000.0000
$#      p9       p10
 3500.0000 4500.0000
```

*MAT_010

```
*MAT_ELASTIC_PLASTIC_HYDRO_SPALL
$ Material Type 10 (units: Newtons-millimeter-millisecond-MPa)
$---+----1----+----2----+----3----+----4----+----5----+----6----+----7----+----8
$      MID        RO         G      SIG0        EH        PC        FS     CHARL
         3   2.30E-3   11.58E3      9.46       0.0      -1.0
$       A1        A2     SPALL
      2.24    -0.012       3.0
$     EPS1      EPS2      EPS3      EPS4      EPS5      EPS6      EPS7      EPS8

$     EPS9     EPS10     EPS11     EPS12     EPS13     EPS14     EPS15     EPS16

$     ES1        ES2       ES3       ES4       ES5       ES6       ES7       ES8

$     ES9       ES10      ES11      ES12      ES13      ES14      ES15      ES16

$---------------------------  EOS-8 CARDS  ------------------------------------
$ Generated EOS 8 (Tabulated Compaction)
*EOS_Tabulated_Compaction
$    EOSID     Gamma        E0      Vol0
         3 0.000E+00 0.000E+00 1.000E+00
$    VolStrain01     VolStrain02     VolStrain03     VolStrain04     VolStrain05
  0.00000000E+00 -1.50000000E-03 -4.30000000E-03 -1.01000000E-02 -3.05000000E-02
$    VolStrain06     VolStrain07     VolStrain08     VolStrain09     VolStrain10
 -5.13000000E-02 -7.26000000E-02 -9.43000000E-02 -1.74000000E-01 -2.08000000E-01
$     Pressure01      Pressure02      Pressure03      Pressure04      Pressure05
  0.00000000E+00  2.23143683E+01  4.86453230E+01  7.81002892E+01  1.48390549E+02
$     Pressure06      Pressure07      Pressure08      Pressure09      Pressure10
  2.23813114E+02  3.17533462E+02  4.85783799E+02  2.83615622E+03  4.33791321E+03
$            Multipliers of Gamma*E
  .000000000E+00  .000000000E+00  .000000000E+00
  .000000000E+00  .000000000E+00  .000000000E+00
$     BulkUnld01      BulkUnld02      BulkUnld03      BulkUnld04      BulkUnld05
  1.48762456E+04  1.48762456E+04  1.50845130E+04  1.58432015E+04  1.88482031E+04
$     BulkUnld06      BulkUnld07      BulkUnld08      BulkUnld09      BulkUnld10
  2.18680810E+04  2.48730826E+04  2.71491481E+04  6.10818643E+04  7.43812278E+04
$-----------------------------------------------------------------------------
```

*MAT_016

```
*MAT_PSEUDO_TENSOR
$#     mid        ro         g        pr
         3  2.120E-3         0     0.200
$#    sigf        a0        a1        a2       a0f       a1f        b1       per
     3.200         8     0.333    0.0104     3.200     1.500     1.250     0.000
$#      er       prr      sigy      etan       lcp       lcr
     0.000     0.000     0.000     0.000         0         0
$#      x1        x2        x3        x4        x5        x6        x7        x8
     0.000 8.6200E-6 2.1500E-5 3.1400E-5 3.9500E-4 5.1700E-4 6.3800E-4 7.9800E-4
$#      x9       x10       x11       x12       x13       x14       x15       x16
 9.6700E-4  0.001410  0.001970  0.002590  0.003270  0.004000  0.004790     0.909
$#     ys1       ys2       ys3       ys4       ys5       ys6       ys7       ys8
  0.309000  0.543000  0.840000  0.975000  1.000000  0.790000  0.630000  0.469000
$#     ys9      ys10      ys11      ys12      ys13      ys14      ys15      ys16
  0.383000  0.247000  0.173000  0.136000  0.114000  0.086000  0.056000     0.000
$ Generated EOS 8 (Tabulated Compaction)
*EOS_Tabulated_Compaction
$    EOSID     Gamma        E0      Vol0
         8 0.000E+00 0.000E+00 1.000E+00
$    VolStrain01     VolStrain02     VolStrain03     VolStrain04     VolStrain05
  0.00000000E+00 -0.43020000E-03 -0.68000000E-01 -0.10000000E-00  0.00000000E-00
$    VolStrain06     VolStrain07     VolStrain08     VolStrain09     VolStrain10
  0.00000000E-00  0.00000000E-00  0.00000000E-00  0.00000000E-00  0.00000000E-00
$     Pressure01      Pressure02      Pressure03      Pressure04      Pressure05
  0.00000000E+00  0.64000000E+01  0.26590000E+03  0.57310000E+03  0.00000000E+00
$     Pressure06      Pressure07      Pressure08      Pressure09      Pressure10
  0.00000000E+00  0.00000000E+00  0.00000000E+00  0.00000000E+00  0.00000000E+00
$             Multipliers of Gamma*E
  .000000000E+00  .000000000E+00  .000000000E+00
  .000000000E+00  .000000000E+00  .000000000E+00
$     BulkUnld01      BulkUnld02      BulkUnld03      BulkUnld04      BulkUnld05
  1.48800000E+04  1.48800000E+04  1.48800000E+04  1.48800000E+04  0.00000000E+00
$     BulkUnld06      BulkUnld07      BulkUnld08      BulkUnld09      BulkUnld10
  0.00000000E+00  0.00000000E+00  0.00000000E+00  0.00000000E+00  0.00000000E+00
```